

# FLUID ANALYSIS AND OPTIMIZATION DESIGN OF SPRAYING PIPE OF INTEGRATED PUMPING AND DISCHARGING FERTILIZER TRUCK

## 抽排一体式施肥车洒水管流体分析及优化设计

Bingchuan BIAN, Tao SONG <sup>\*) 1</sup>

College of mechanical and architectural engineering, Taishan University, Taian, Shandong/ China

Tel: +8605386711808; E-mail: stsong925@163.com

Corresponding author: Tao Song

DOI: <https://doi.org/10.35633/inmateh-68-14>

**Keywords:** *Sprinkler pipe, simulation platform, fluid pressure, fluid velocity, flow trace number*

### ABSTRACT

According to the flow calculation, the basic structure of the sprinkler pipe of the integrated suction and drainage fertilizer truck was designed. Based on the 3D CAD / CAE Software SolidWorks / flow simulation platform, the structural models of three kinds of sprinkler pipes with different layout forms of outlet pipes were established, and the fluid analysis was carried out. According to the distribution of pressure, velocity and flow trace number in the tube, the optimal structure was obtained.

### 摘要

根据流量计算设计了抽排一体式施肥车洒水管的基本结构，并基于三维CAD/CAE软件SolidWorks/ Flow simulation 平台，建立出水管不同布置形式的三种洒水管的结构模型，进行流体分析。并根据管内的压力、速度和流动迹线数的分布，得出了最优结构。

### INTRODUCTION

The integrated pumping and discharging fertilizer truck is suitable for sucking and transporting from septic tank to rural land, and spraying manure, sewage, and all fluid and semi-fluid substances to the land. The basic principle of fertilizing vehicle is to use engine power to drive the on-board pumping and discharging integrated pump through the power output device connected to the gearbox, so as to realize the suction and discharge of liquid fertilizer. The integrated pumping and discharging fertilizer vehicle is mainly composed of chassis, diesel engine, integrated pump, suction pipeline system, spraying pipeline system and control system. Among them, how to design the structure of the spraying pipeline can ensure that the flow of each branch pipe is equal when the main pipe pressure is equal. Therefore, it is of great significance to the structural design of spraying pipeline.

The research on the spray pipeline system is relatively less, compared with the similar research mainly having the following content.

The spatial pipeline of a power system was studied. The Galerkin method was used to discretize the coupling system composed of conduit and fluid, and the governing equation of the coupling system was established. The finite element method considering the initial stress stiffness is used to numerically calculate the vibration characteristics of the conduit before and after pressurization. The influence of fluid structure interaction on the vibration characteristics of the pipe structure is analysed in detail, and the results are compared with the experimental results (Chen, 2007).

The researchers analysed the fluid structure coupling phenomenon of pressure pipeline, established the finite element mathematical model of fluid solid coupling, used the finite element software ADINA to simulate the transition process caused by valve opening and closing, carried out numerical simulation calculation on the fluid solid coupling phenomenon of straight pipe pressure pipeline under different constraint conditions, and carried out modal analysis (Feng, 2009).

The researchers studied the cavitation phenomenon in the water pipeline of the heat exchanger test-bed, simulated the cavitation process of the fluid in the pipeline throttling by using the numerical calculation method, and analysed the changes of water content and pressure along the pipeline under different outlet pressure (Zheng, 2011).

<sup>1</sup>Bingchuan Bian, Prof. Ph.D.; Tao Song, associate Prof. Ph.D.

CFD technology to simulate the three-dimensional flow of a flat inlet water jet propulsion system was used. Based on the flow loss, outflow quality and pressure distribution in the inlet pipe, the influence of five different inlet lip angle schemes on the flow performance of the pipeline is compared and analysed (Liu, 2011).

The special water injection pipe was designed. The collar of the water injection pipe adopts the structure of inner boss and special thread structure, so that the inner diameter of the water injection pipe and the coupling is completely consistent, which can effectively eliminate the influence caused by eddy current, prolong the continuous working life of the water injection pipe, increase the water injection volume, increase the formation pressure, and improve the oil recovery. To a certain extent, the frequency of shutdown maintenance is reduced, and the production cost is greatly reduced (Li, 2013).

The researchers simulated and analysed three different types of draft tubes based on CFD technology, and revealed the influence of the pier on the internal flow of the draft tube by comparing the velocity distribution and streamline parameters of the draft tube (Liao, 2016).

The influence of structural parameters of cooling water pump on characteristics and how to adjust it to achieve the desired effect were studied. ANSYS CFX was used to analyse the flow field of cooling water pumps with different structures to obtain corresponding data for comparative analysis (Feng, 2017).

The researchers established a variety of finite element simulation models with different parameters of pipe wall thickness, length, inner diameter and material using ANSYS Workbench analysis software, and analysed the stress-strain characteristics of pipe wall under internal pressure in detail (Yan, 2018).

The authors studied the characteristics of velocity field and pressure field of the pressure pipe of tea cleaning machine by means of CFD fluid analysis and simulation software combined with the relevant basic theory of fluid mechanics. By comparing three different sizes of circulating pipes, the influence of different sizes on the pressure field distribution of circulating pipelines is obtained (Yu, 2019).

The researchers introduced the main functions of the Fluid Simulation Software SolidWorks flow simulation by simplifying the modelling of the hot air pipeline of rotary kiln and simulating the air flow in the pipeline, and analysed the structural design of the hot air pipeline of the rotary kiln (Zhang, 2019).

The authors used COMSOL Multiphysics software to simulate the fluid dynamics of pipelines with different leakage apertures, so as to analyse the pressure and flow variation law of leakage pipelines and leakage openings (Wang, 2020).

The computer model was developed to simulate pressure and flow rate distribution along pipes and laterals of pressurized irrigation systems in operation were studied. The software runs in a Windows environment and is capable of simulating irrigation systems having multiple pump stations combined in series and/or in parallel, booster pump stations, parallel pipes and looping pipes (C.de L.T. de Andrade, 1999).

The analysis and optimization of a liquamatic fire water monitor with a novel self-swinging mechanism were presented. The design of the self-swinging mechanism has adopted a four-bar linkage driven by an impeller. The Fluent software was used to simulate the internal flow performance of the fire water monitor. In particular, the effects of the cross-sectional shape, diameters of the monitor body, inlet water pressure, and drive set of the self-swinging mechanism on the jet characteristics were analysed (Hu, 2012).

An optical particle tracking velocimetry (PTV) technique is proposed in this paper to determine drop velocity, diameter and angle. The technique has been applied to the drops emitted by an isolated impact sprinkler equipped with two nozzles (diameters 3.20 and 4.37 mm) operating at a pressure of 175 kPa (Bautista Capetillo, 2014).

The pipes made of plastic materials are generally used in pipelines and the laterals of irrigation systems. Plastic materials such as polyethylene allow significant changes in pipe cross section due to operating pressure, but traditional equations used for determining head loss do not account for this effect. The purpose of this research was to develop an equation for determining friction head loss along elastic pipes (O. Rettore Neto, 2014).

The optimal design of sprinkler irrigation systems is a complicated nonlinear programming problem that is related to the performance of the system and meanwhile an economic problem to farmers in developing countries. Ant colony optimization (ACO), a meta-heuristic algorithm with the strategies inspired by foraging ants, was considered. Exactly an Ant Cycle System was proposed to solve this problem. The performance of ACO was compared to that of Genetic Algorithm (GA), and the optimal results were further validated by field tests on four small-scale irrigation systems (Qin, 2015).

The dynamical interaction between solids and fluids is a subject of paramount importance in Mechanics with a wide range of applications to engineering problems. It is, however, still a challenging topic of theoretical investigation.

With a view to case studies of dynamical behaviour of rockets, turbines, jets and sprinklers, a treatment was developed that, in the full respect of the principle of conservation of mass and under suitable simplifying assumptions, leads to evaluate the thrusting force exerted by the fluid on the solid (Giovanni Romano, 2017).

A multi-objective optimization of a flow straightener in a firefighting water cannon is performed by using the surrogate modelling and a hybrid multi-objective genetic algorithm to increase the jet range of the water cannon. Based on analysis using the three-dimensional Reynolds-averaged Navier-Stokes equations, the optimization is carried with a surrogate model and the radial basis neural network (Xiang, 2019).

One of the important parameters in developing dry ice blasting nozzle is the high-speed dry ice pellets. However, many studies focus primarily only on its performance without considering the noise emission that comes from an operating nozzle. In this method, the central composite optimization tool has been used. The two-way mass momentum and energy exchange are successfully modelled using the two-way mass momentum model. As an attempt to theoretically verify the model accuracy, a comparison is conducted on the density, pressure, temperature, as well as Mach number ratios corresponding to various ratios of nozzle area (Mohamad Nur Hidayat Mat, 2021).

In this paper, the three-dimensional basic finite element model of the spraying pipe of the integrated pumping and drainage fertilizer truck is established on the platform of SolidWorks / flow simulation. On the basis of fluid finite element analysis, the layout of spray pipe joint is optimized, and a good conclusion is obtained, which has certain reference significance for actual production.

## MATERIALS AND METHODS

### **Mathematical model of spraying pipe of fertilizer truck pipeline parameter design**

It is known that the diameter of the main pipe is D104 mm / D114 mm, the internal pressure is 0.15 MPa, the ambient temperature is 20° and the liquid velocity in the main pipe is  $V_1 = 1$  m/s, and the total length is  $L = 1000$  mm. Two pipes are arranged around, and one pipe can be calculated by calculation formula.

The diameter of the branch pipe is designed according to the known conditions.

According to the section average velocity  $V$  and cross-section area  $a$ , the flow rate is as follows:

$$Q = VA \quad (1)$$

Then the flow rate of the main pipe is equal to the sum of the flow rate of the branch pipe, and the following formula is established:

$$Q_1 = Q_2 \quad (2)$$

There are:

$$V_1 A_1 = n V_2 A_2 \quad (3)$$

Where  $V_1$  is the average cross-section velocity of the main pipe;  $A_1$  is the cross-sectional area of the main pipe;  $n$  is the number of branch outlets;  $V_2$  is the average flow velocity of the branch section;  $A_2$  is the cross-sectional area of the main pipe.

### **Establishment of mathematical model calculation of Reynolds**

The Reynolds number of the fluid in a circular pipe is calculated according to the parameters of the known liquid.

$$Re = \frac{\rho V d}{\mu} \quad (4)$$

Where  $\rho$  is the density of the liquid, calculated according to the density of water,  $\rho = 1000$  kg/m<sup>3</sup>;  $V$  is the average velocity;  $D$  is the characteristic length (m), where  $D$  is the diameter of the circular pipe through which the fluid flows;  $\mu$  is the viscosity of the fluid, and the viscosity of water at 20°C is  $\mu = 0.001$  Pa.s. The critical Reynolds number of the tube is 2300.

If the above parameters are substituted into formula (4), then:

$$Re = \frac{\rho V d}{\mu} = 104000 > Re_{cr} = 2300 \quad (5)$$

It can be seen from the above formula that the fluid in the pipe is turbulent with high Reynolds number.

**Mach number calculation**

Mach number is the ratio of the characteristic velocity of a fluid to the velocity of sound in the fluid. It is mainly used to measure the compressibility of a fluid.

$$Ma = \frac{V}{C} = \frac{1}{1500} \approx 6.667 \times 10^{-4} < 0.3 \tag{6}$$

Where  $C$  is the velocity of sound propagating in the fluid,  $C = 1500$  m/s. According to the above formula, it can be concluded that this fluid is low Mach number fluid flow, and the liquid is incompressible fluid with constant density.

**Problem solving**

The Reynolds averaged Navier Stokes equations (RANS equations) are used to solve the fluid motion in water pipes. For Newtonian fluids, the following results are obtained:

$$\rho \left( \frac{\partial \mathbf{u}}{\partial t} + \mathbf{u} \cdot \nabla \cdot \mathbf{u} \right) = -\nabla P + \nabla \cdot \left( \mathbf{u} \left( \nabla \cdot \mathbf{u} + (\nabla \cdot \mathbf{u})^T \right) - \frac{2}{3} \mu (\nabla \cdot \mathbf{u}) \mathbf{I} \right) \tag{7}$$

$\rho$  is the density of the liquid (kg/m<sup>3</sup>);  $\mathbf{u}$  is the velocity of the fluid (m/s);  $t$  is the time (s);  $P$  is the fluid pressure (Pa);  $T$  is the temperature (K);  $\mu$  is the hydrodynamic viscosity (Pa.s);  $I$  is the Prandtl mixing length (m).

**RESULTS**

**Fluid numerical analysis**

The three-dimensional finite element model of sprinkler pipe of suction and drainage integrated fertilizer truck was established by using SolidWorks / flow simulation software, as shown in Figure 1, and the fluid analysis was carried out. The upper branch pipe at the right end is the fluid inlet, and the left and right sides of the horizontal main pipe are all closed. The thermal condition of the wall is adiabatic and the roughness is 12.5  $\mu\text{m}$ .

According to the length of the main pipe, 11 thin tubes on the horizontal main pipe are fluid outlets, and the outlet spacing is evenly distributed. The distance of the branch pipe is  $L = 80$  mm,  $n = 11$ , and the flow rate of liquid in the branch pipe is  $V_1 = 1.25$  m/s. Substituting the parameters into equation (3), the following results are obtained:

$$1 \times \pi \times 52^2 = 11 \times 1.25 \times \pi r_2^2 \tag{8}$$

where  $r_2$  is the radius of branch pipe,  $r_2 = 14.023$  mm, so after rounding, the diameter of nozzle outlet pipeline is  $D=28$  mm /  $d=34$  mm. The nozzle outlet pressure is set to the ambient pressure and set to 0.10325 MPa.

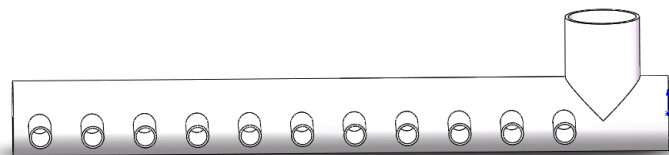


**Fig. 1 - Three dimensional model of sprinkler pipe with uniform outlet pipe**

The global grid is selected for grid division. After 70 iterations, the flow traces are set as 50, and the baseline diameter is 2 mm. The cloud chart and flow trace of pressure calculation results are shown in Fig. 2, and the nephogram and flow trace of water flow velocity are shown in Fig. 3. The distribution of flow trace number of uniform distribution structure of outlet pipe is shown in Table 1.

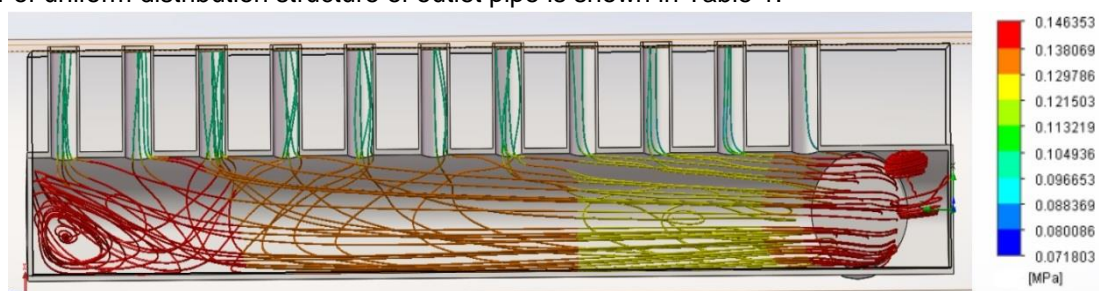


**Fig. 2 - Pressure nephogram and flow trace of uniform distribution structure of outlet pipe**

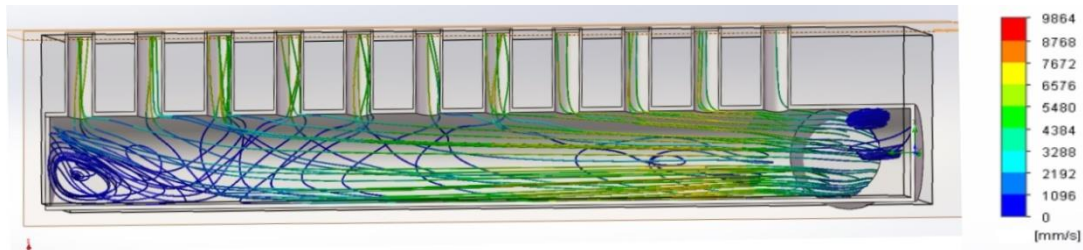


Fig. 3 - Water pipe velocity distribution and flow of uniform distribution structure of outlet pipe

It can be seen from Figure 2 that the water pressure at the inlet of the main pipe is the maximum, and the water pressure gradually decreases with the flow to the middle, and increases to the initial value when it reaches the end of the left main pipe. At the same time, the water pressure at the outlet is lower than that at the inlet. It can be seen from Fig.3 that the water flow velocity at the inlet of the main pipe is the maximum, and the water flow velocity gradually decreases with the flow towards the middle. When it reaches the end of the left main pipe, the flow velocity drops to the lowest; the vortex velocity at the left and right ends of the main pipe is the lowest; at the same time, the water flow velocity at the outlet is lower than that at the inlet.

Table 1

Distribution of the number of flow traces in the uniform structure of outlet pipe

Serial number of outlet pipe (from left to right)	1	2	3	4	5	6	7	8	9	10	11	loss
Number of flow traces	5	4	8	5	5	3	5	2	3	3	1	6

It can be concluded from table 1 that the largest number of flow traces is 8, and the third exit from left to right is 700 cm away from the entrance centre; the least number of flow traces is 1, 60 cm away from the entrance centre, and the number of flow traces at the 8th, 9th and 10th is very small, so the distance is obtained; the number of flow traces is lost by 6, and the loss rate is 12%.

It can be concluded from the above that the number of flow traces in the three-dimensional model with uniform distribution of outlet pipe is more in the distance from the inlet, and less in the near area, that is, the far flow rate is larger, the near flow rate is small, the flow trace loss rate is 12%, and the flow trace efficiency is 88%, which is mainly manifested in the formation of vortices on the left and right sides of the main pipe. It can be concluded from the above that the efficiency of this kind of structure is low, and the flow rate of each outlet is uneven, which affects the average of fertilization effect.

**Structural calculation of outlet**

Modify the three-dimensional finite element model of sprinkler pipe of fertilizer truck, reduce the number of outlet pipes to 8, start from the main inlet pipe according to the spacing, start from 80 mm, increase by 10 mm each time, and increase until the spacing is 140 mm. The other boundary conditions are analysed as shown in Fig. 4.

Take  $n = 8$ , where  $r_2$  is the radius of the branch pipe, and its size remains unchanged,  $r_2 = 14$  mm.

$$1 \times \pi \times 52^2 = 8 \times V_1 \times \pi r_2^2 \tag{9}$$

The results show that the velocity of liquid in the branch pipe is  $V_1 = 1.72$  m/s, the number of branch pipes decreases and the velocity increases. The nozzle outlet pressure is set to the ambient pressure and set to 0.10325 MPa.

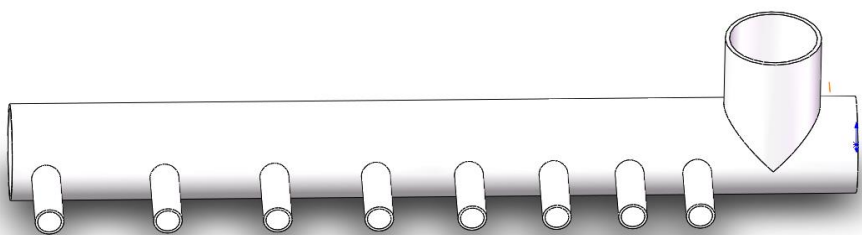


Fig. 4 - Three dimensional model of the structure in which the distribution distance of the outlet pipe increases gradually from the inlet

The global grid is selected for grid division. After 67 iterations, the flow trace is set as 50, and the baseline diameter is 2 mm. The pressure calculation results and flow trace are shown in Fig. 5, and the flow velocity nephogram and flow trace are shown in Fig. 6. The distribution of outlet pipe gradually increases from the inlet, and the structure flow trace distribution is shown in Table 2.

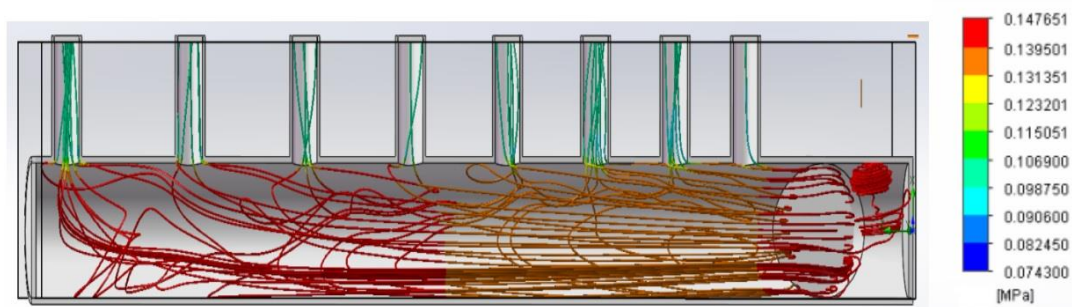


Fig. 5 - Pressure nephogram and flow trace of 3D model with the distribution distance of outlet pipe gradually increasing from the inlet

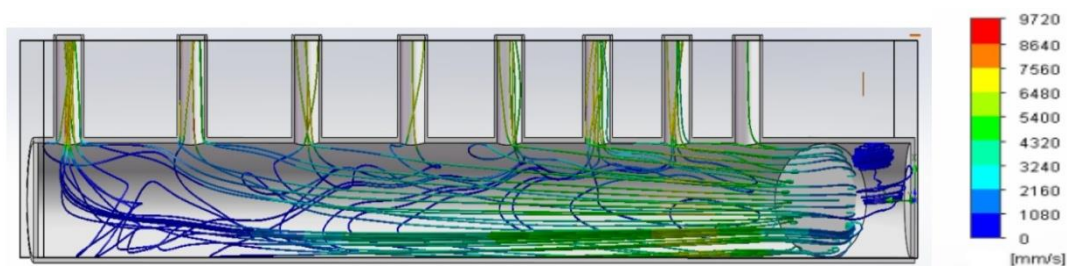


Fig. 6 - Water flow velocity nephogram and flow trace of 3D model with the distribution distance of outlet pipe gradually increasing from the inlet

It can be seen from Fig. 5 that the water pressure at the inlet of the main pipe is the maximum, and the water pressure gradually decreases with the flow to the middle. When it reaches half of the main pipe on the left, the water pressure increases to the initial value. At the same time, the water pressure at the outlet is lower than that at the inlet. It can be seen from Fig. 6 that the water flow velocity at the inlet of the main pipe is the maximum, and with the flow speed gradually decreasing towards the middle, the water flow speed will be the lowest when reaching the end of the left main pipe; there is no eddy current at the left end of the main pipe, and the vortex velocity at the right end is the lowest; at the same time, the water flow velocity at the outlet is lower than that at the inlet.

Table 2

Distribution of water outlet pipe gradually increases from the water inlet to the structure flow trace distribution

Serial number of outlet pipe (from left to right)	1	2	3	4	5	6	7	8	loss
Number of flow traces	14	5	4	2	5	9	6	1	4

It can be concluded from table 2 that the largest number of flow traces is 14, which is at the exit of the first leftmost end, 860 cm away from the entrance centre; the number of flow traces at the eighth outlet is the least, which is 1, 60 cm away from the inlet centre; 4 flow traces are lost, with a loss rate of 8%.

It can be concluded that the distribution of outlet pipe gradually increases from the inlet, and the number of flow traces in the structure model is further from the inlet, and the number is the least close to the entrance. It also shows that the far flow is larger and the near flow is smaller. The loss rate of the flow trace is 8%, and the effective rate of the flow trace is 92%. It can be concluded from the above that the efficiency of this structure is better than that of uniform distribution structure, but there are also vortices, the efficiency is not high, and each outlet flow is not uniform, which will affect the average of fertilization effect.

**The distribution of water outlet pipe**

Modify the three-dimensional finite element model of sprinkler pipe of fertilizer truck, reduce the number of outlet pipes to 8, start from the main inlet pipe according to the spacing, start from 140 mm, decrease by 10 mm each time, and increase until the spacing is 80 mm and carry out fluid analysis, as shown in Fig. 7. Other boundary conditions remain unchanged and other parameters are the same as those in Fig. 1.

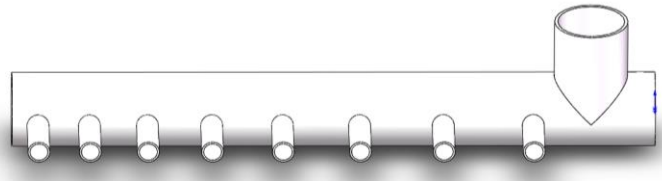


**Fig. 7 - 3D model of structure in which the distribution distance of outlet pipe gradually decreases from the inlet**

The global grid is selected for grid division. After 72 iterations, the flow trace is set as 50, and the baseline diameter is 2 mm. The pressure calculation results and flow trace are shown in Fig. 8, and the flow velocity nephogram and flow trace are shown in Fig. 9.

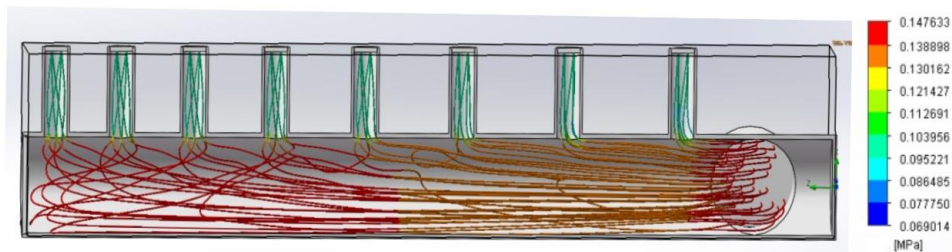


**Fig. 8 - Pressure nephogram and flow trace of 3D structure model with the distance of outlet pipe decreasing gradually from inlet**

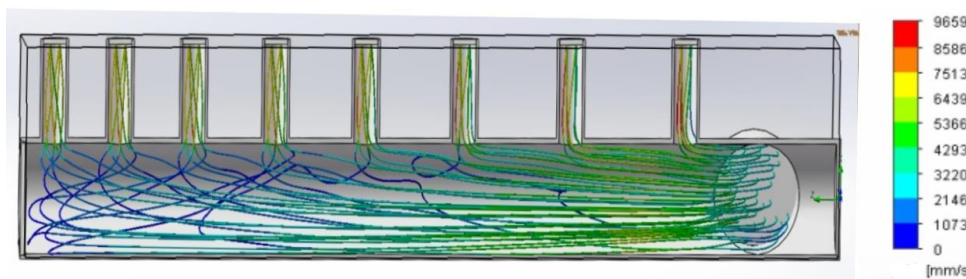


**Fig. 9- Flow velocity nephogram and flow trace of 3D model with outlet pipe decreasing gradually from inlet**

It can be seen from Fig. 8 that the water pressure at the inlet of the main pipe is the maximum, and the water pressure gradually decreases with the flow to the middle. When it reaches half of the main pipe on the left, the water pressure increases to the initial value. At the same time, the water pressure at the outlet is lower than that at the inlet. It can be concluded from Figure 9 that the water flow velocity at the inlet of the main pipe is the largest, and the flow velocity decreases gradually with the middle flow. When it reaches the end of the left main pipe, the flow velocity will be reduced to the lowest; there is no eddy current at the left end of the main pipe; meanwhile, the water flow velocity of the outlet is lower than the water velocity of the inlet.

**Table 3**

**The distribution of outlet pipe gradually reduces the number of structural flow trace from the inlet**

<b>Serial number of outlet pipe (from left to right)</b>	1	2	3	4	5	6	7	8	Loss
<b>Number of flow traces</b>	6	6	6	6	6	6	7	7	0

It can be concluded from table 3 that the highest number of flow traces is 7, which is at the 7th and 8th outlet pipe of the rightmost end, 60 cm away from the inlet centre; the number of flow traces of other outlet pipes are the same, all of them are 6; the number of flow traces is 0, and the loss rate is 0%.

It can be concluded that the number of flow traces of this structural model is relatively average, which also shows that the flow rate of each outlet is almost equal, the loss rate of flow trace is 0%, indicating that the flow efficiency is 100%, and there is no vortex on the left and right sides of the main pipe. To sum up, this kind of structure has the highest efficiency, the average flow rate of each outlet is almost equal, and the fertilization effect is equal, so this structure is finally selected.

## CONCLUSIONS

1) Fluid numerical analysis shows that the sprinkler pipe is an important part in the design and manufacturing process of the fertilizer truck. The design of the fertilizer truck mainly focuses on the main pipe size design of the sprinkler pipe and the size design and distribution design of the outlet pipe orifice.

2) Structural calculation of outlet show that the spraying speed and uniformity of liquid fertilizer can be improved effectively by reasonably arranging the position, quantity and diameter of the outlet pipe.

3) The distribution analysis of water outlet pipe shows that the application of fluid finite element analysis method in the design of sprinkler pipe of suction and drainage integrated fertilizer truck can effectively improve the design quality of sprinkler pipe, reduce the blindness in sprinkler design, and improve the economy and accuracy of product design.

## ACKNOWLEDGEMENTS

We acknowledge that this work was financially supported by the Shandong Major Agricultural Application Technology Innovation Project "Research, development and integration demonstration of key equipment for rural toilet waste treatment and utilization (No.SD2019NJ017)".

## REFERENCES

- [1] C. de L.T. de Andrade., R. G. Allen., (1999). SPRINKMOD pressure and discharge simulation model for pressurized irrigation systems. Model development and description. *Irrig Sci*, Issue 18, pp. 141-148, New York / United States.
- [2] Capetillo C.B., Robles O., Salinas H., Playán E., (2014). A particle tracking velocimetry technique for drop characterization in agricultural sprinklers. *Irrig Sci*, Issue 32, pp. 437-447, New York / U.S.A.
- [3] Chen X., Zhou W., (2007). Vibration characteristic analysis of pressure pipes with fluid-structure interaction (压力管道流固耦合振动特性分析). *Journal of Rocket Propulsion*, Vol. 33, Issue 5, pp. 27-31, Xian / China.
- [4] Feng W., Song L., Xiao G., (2009). Coupling analysis of fluid-structure interaction in pressure pipes based on ADINA (基于 ADINA 的压力管道流固耦合分析). *Engineering Journal of Wuhan University*, Vol. 42, Issue 2, pp. 264-267, Wuhan / China.
- [5] Hu G., Long M., Liang J., Li W., (2012). Analysis of jet characteristics and structural optimization of a liquamatic fire water monitor with self-swinging mechanism. *International Journal Advanced Manufacturing Technology*, Issue 59, pp.805-813, Guildford / England.
- [6] Giovanni R., Raffaele B., Marina D., (2017). Solid-fluid interaction: a continuum mechanics assessment. *Acta Mech*, Issue 228, pp. 851-869, Wien / Austria.
- [7] Liao R., (2016). Analysis of the influence of diaphragm pier on the stability of flow in draft tube (隔墩对尾水管内部水流运动稳定性影响分析). *Yangtze River*, Issue 47, pp. 116-119, Wuhan / China.
- [8] Liu R., Huang G., (2011). Numerical study on effect of inlet lip on hydrodynamics for water jet propulsion (入口唇角对喷水管道流动性能影响的数值分析). *Ship Building of China*, Vol. 52, Issue 1, pp. 39-46, Shanghai/China.
- [9] Li S., Li S., Qin S., (2013). Research and application of water injection pipe with new connection mode (新型连接方式注水管的研制与应用). *Manufacturing informatization*, Issue 4, pp. 111-114, Jiangsu/China.
- [10] Mohamad N.H.M., Asmuin N.Z., Basir M.F., Mohammad R.S., Mohd S.M.K., Taufiq K.A.K., Marjan G., (2021). Optimizing nozzle convergent angle using central composite design on the particle velocity and acoustic power level for single-hose dry ice blasting nozzle. *Journal of Thermal Analysis and Calorimetry*, Issue 144, pp. 2159-2173, Dordrecht / Hungary.



- [11] Neto O.R., Botrel T.A., Frizzone J. A., Camargo A.P., (2014). Method for determining friction head loss along elastic pipes. *Irrig Sci*, Issue 32, pp. 329–339, New York/United States.
- [12] Tu Q., Li H., Wang X., Chen C., (2015). Ant colony optimization for the design of small-scale irrigation systems. *Water Resources Manage*, Issue 29, pp. 2323-2339, Beijing/China.
- [13] Wang W., Guo J., Zhou C., Zhang J., Huang J., Yao W., (2020). COMSOL Fluid simulation analysis of urban water supply pipeline leakage (城市供水管道泄漏的 COMSOL 流体仿真分析). *China Municipal Engineering*, Issue 2, pp. 36-41, Shanghai/China.
- [14] Xiang Q., Xue L., Kim KwangYong., Shi Z., (2019). Multi-objective optimization of a flow straightener in a large capacity firefighting water cannon (大容量火灾中流动矫直机的多目标优化). *Journal of Hydrodynamics*, Vol 31, Issue 1, pp. 137-144, Shanghai/China.
- [15] Yan Z., Chen G., Xu C., (2018). Simulation study on stress and strain characteristics of fluid pipeline based on finite element model (基于有限元模型的流体管道应力应变特性仿真实验研究). *Research and Exploration in Laboratory*, Vol 37, Issue 7, pp. 110-114, Beijing /China.
- [16] Yu P., Gao T., Li M., (2019). Design and optimization of pressure pipe of tea cleaning machine based on CFD fluid analysis technology (基于 CFD 流体分析技术的茶叶清洗机压力管道设计与优化). *Journal of Baoshan University*, Vol 38, Issue 5, pp. 27-31, Yunnan/China.
- [17] Zhang B., (2019). Simulation and analysis of rotary kiln hot air pipeline based on SolidWorks (基于 CFD 流体分析技术的茶叶清洗机压力管道设计与优化). *Modern metallurgy*, Vol 47, Issue 5, pp. 60-62, Jiangsu/China.
- [18] Zheng C., Zheng Q., Zhou D., Zan S., Sun Y., (2011). Numerical simulation on cavitation of throttle pipe in heat exchanger test-bed (换热器试验台节流管道气蚀现象数值模拟分析). *Refrigeration Air Conditioning & Electric Power Machinery*, Vol 32, Issue 2, pp. 12-15, Zhejiang/China.
- [19] Zhu Y., Tang L., XU L., Peng K., Zhang Z., (2017). Design and simulation of wheel foot structure of a composite robot (一种复合式机器人的轮足结构设计及仿真). *Equipment Manufacturing Technology*, Issue 10, pp. 26-28, Guangxi /China.